

Dehydration of aldoximes on rare earth exchanged (La^{3+} , Ce^{3+} , RE^{3+} , Sm^{3+}) Na–Y zeolites: A facile route for the synthesis of nitriles

Bejoy Thomas · S. Sugunan

Received: 10 January 2006 / Revised: 29 May 2006 / Published online: 26 January 2007
© Springer Science+Business Media, LLC 2007

Abstract Rare earth exchanged Na–Y zeolites, H-mordenite, K-10 montmorillonite clay and amorphous silica-alumina were effectively employed for the continuous synthesis of nitriles. Dehydration of benzaldoxime and 4-methoxybenzaloxime were carried out on these catalysts at 473 K. Benzonitrile (dehydration product) was obtained in near quantitative yield with benzaldoxime whereas; 4-methoxybenzaloxime produces both Beckmann rearrangement (4-methoxyphenylformamide) as well as dehydration products (4-methoxy benzonitrile) in quantitative yields. The production of benzonitrile was near quantitative under heterogeneous reaction conditions. The optimal protocol allows nitriles to be synthesized in good yields through the dehydration of aldoximes. Time on stream (TOS) studies show decline in the activity of the catalysts due to neutralization of acid sites by the basic reactant and product molecules and water formed during the dehydration of aldoximes.

Keywords Beckmann rearrangement · Benzaldoxime · Benzonitrile · 4-Methoxybenzaloxime · 4-Methoxybenzonitrile · 4-Methoxyphenylformamide · Rare earth exchanged Na–Y zeolites

1 Introduction

The acid amount and thermal stability of synthetic Na–Y zeolite can be dramatically improved by ion exchanging with rare earth metal cations, and the amount of improvement is controlled by the extent of cation exchange [1, 2]. These zeolites have been extensively used for industrial applications. Lanthanum exchanged Na–Y zeolite plays an important role in the preparation of catalysts for fluid catalytic cracking (FCC), one of the most widely applied petroleum refining processes that makes use of zeolite catalyst components [2, 3]. Rare earth cations play an important part in determining the steady state conformation of Y zeolite during catalytic cracking. During the regeneration of FCC unit, the catalyst is exposed to high-temperature which dealuminates the zeolite framework, reducing the number of Brønsted acid sites (BAS). However, dealumination can only occur at Si–O–Al sites containing protons as cations, rare earth cations effectively prevent dealumination. Also, these zeolites have been extensively used as catalysts for a large number of industrially important reactions such as isomerization [4, 5], alkylation [5–7] and Beckmann rearrangement [8].

Aromatic nitriles constitute a key component of numerous commercial compounds including pharmaceuticals, agrochemicals, pigments, and dyes [9]. Their utility also stems from the numerous possible nitrile transformations, including the synthesis of benzoic acid, amidines, imidoesters, benzamidines, amines, heterocycles and aldehydes [10, 11]. Many important multi-step synthetic reactions pass through a nitrile intermediate. Examples include the synthesis of ibuprofen and ketoprofen; two widely used pharmaceutical

B. Thomas · S. Sugunan (✉)
Department of Applied Chemistry, Cochin University of
Science and Technology, Kochi 682 022, India
e-mail: ssg@cusat.ac.in

Present Address:
B. Thomas
NMR Research Center, Indian Institute of Science,
Bangalore 560 012, India
e-mail: bjoy@sif.iisc.ernet.in

was supplied by *Zeolyst International*, New York, USA. K-10 montmorillonite clay was procured from *Aldrich Chemical Company*, USA. Amorphous silica-alumina was prepared by known chemical methods [38, 39]. Benzaldehyde, 4-methoxybenzaldehyde, hydroxylamine hydrochloride, sodium bicarbonate, benzene and acetonitrile were purchased from *S-D-Fine Chemicals*, India and used without further purification.

2.2 Physicochemical characterization

Elemental analysis of the samples was done on a *JEOL JSM-840 A* (Oxford make model No. 16211 with a resolution of 1.3 eV) EDX analyzer. Samples were prepared by dusting the zeolite powder onto a double sided carbon tape mounted on a metal stub. It was then sputter coated with a thin film of gold to reduce charging effects and a minimization procedure was adopted to calculate the exact metal ion concentration [40]. The infrared induced vibrations of the samples were recorded using a *Nicolet Impact 400FT* Infrared Spectrometer using KBr pellet technique. The crystalline nature of the materials was established by X-ray diffraction studies performed using a *Rigaku D-max C* X-ray diffractometer with Ni-filtered Cu K α radiation in an angular range of 2θ from 5 to 40°. Solid-state NMR experiments were carried out over a *Bruker DSX-300* spectrometer at resonance frequencies of 78.19 MHz for ^{27}Al , 59.63 MHz for ^{29}Si and 79.97 MHz for ^{23}Na . For all the experiments a standard 4 mm double-bearing *Bruker* MAS probe was used. A sample rotation frequency of 8 kHz for ^{23}Na , 7 kHz for ^{27}Al and ^{29}Si with a single pulse excitation corresponding to $\pi/2$ flip angle were used. The 90° pulses for sodium-23, ^{27}Al and ^{29}Si were 5.5, 6 and 10 μs respectively whereas the relaxations delays were 0.5, 2 and 10 s. The assessment of surface acidity was done by temperature programmed desorption of ammonia (NH_3 -TPD). TPD was performed using conventional equipment with a detector for sensing ammonia. Simultaneous determination BET surface area and pore volume were performed on a *Micromeritics Gemini* surface area analyzer using N_2 adsorption technique at liquid nitrogen temperature. The pore volume was calculated up to a relative pressure of 0.9976.

2.3 Catalytic reaction procedure

Catalytic reactions were carried out in a fixed-bed, down-flow reactor with 0.6 cm internal diameter and 30 cm height. Catalysts (700 mg) were activated for 12 h in the presence of oxygen, allowed to cool to room temperature under a steady flow of dry nitrogen and

then heated to reaction temperature where it was kept for 1 h before the commencement of the reaction. The reaction mixture [5% (w/v) solution of oximes in a 1:1 mixture of benzene acetonitrile] was fed into the reactor at a flow rate of 4 mL/h (weight hourly space velocity (WHSV); 0.29 h^{-1}) in presence of dry N_2 . Products were collected after 2 h of reaction (TOS; 2 h) and analyzed by a *Chemito GC1000* gas chromatograph using an *SE-30* capillary column (oven temperature 353–503 K, injector temp. 373 K, and detector temp. 373 K). The products were further analyzed by a gas-chromatograph-mass spectrometer using a *Shimadzu-5050* spectrometer provided with a 30 m HP-30 capillary column of cross linked 5% phenylmethylsilicone. The MS detector voltage was 1 kV. The m/z values and relative intensity (%) are indicated for the significant peaks. (Column temperature was between 323–533 K with heating rate of 10 K/min, injector: 513 K and detector: 563 K).

3 Results and discussion

3.1 Physicochemical characteristics

The elemental analysis of the rare earth exchanged zeolites showed that the aluminium content was principally unchanged by the ion exchange procedure. The unit cell composition of different zeolite samples is listed in Table 1. Thermal studies on the samples show that the parent and different rare earth exchanged zeolite systems are highly stable at 873 K. X-ray diffraction and infrared spectral studies confirm that the zeolite framework remains intact even after chemical treatment at moderately high temperatures during ion exchange. Consistent with the earlier reports, the parent as well various rare earth exchanged zeolites crystallizes into cubic unit cell with space group F3dm. Fourier Transform infrared spectroscopy shows uniform transmittance patterns for the parent and rare earth exchanged zeolites. Rare earth exchanged zeolites and Na–Y zeolite show bands characteristic of faujasite type of zeolites in the framework region. The spectra show major shifts in the framework vibrations of Na–Y zeolite upon rare earth exchange as evidenced by Table 1. IR spectra and X-ray diffraction measurements showed that rare earth Na–Y zeolites are crystalline and present well-defined structures. The results of the MAS NMR studies on these systems are reported in our earlier communication [41].

2,6-DMP desorption clearly shows the variation of Brønsted acid amount with the exchange of sodium with rare earth metal cations (Table 1). BAS amount

Table 1 Chemical composition, important framework vibrational modes, and the amount of 2,6-DMP desorbed from the parent and different as-exchanged rare earth zeolites

Zeolite	Chemical composition ^a	Assymmetric stretch	Symmetric stretch	Double ring ^c	T–O bend ^d	Amount of 2,6-DMP desorbed ^e (mmol/g)
		(cm ⁻¹) EL or IT ^b	(cm ⁻¹) EL or IT ^b	(cm ⁻¹)	(cm ⁻¹)	
Na–Y	Na _{78.5} Al _{78.5} Si _{113.5} O ₃₈₄	1058	791	571	460	0.18
CeNa–Y	Ce _{10.7} Na _{44.3} Al _{76.4} Si _{115.6} O ₃₈₄	1078	777	578	468	0.74
LaNa–Y	La _{10.5} Na _{45.0} Al _{78.5} Si _{115.5} O ₃₈₄	1073	767	573	465	0.56
RENa–Y ^f	La _{9.38} Ce _{1.21} Pr _{2.72} Nd _{3.10} Na _{27.27} Al _{78.5} Si _{115.5} O ₃₈₄	1074	779	577	468	0.64
SmNa–Y	Sm _{8.1} Na _{52.4} Al _{78.5} Si _{115.5} O ₃₈₄	1073	778	579	469	0.75

^a As determined by Energy Dispersive X-ray analysis

^b EL, External linkage; IT, Internal tetrahedral

^c D6R double ring units

^d T = Si, Al

^e Number of BAS as obtained from thermodesorption studies [TGAQ 50 V_{2.34} thermal analyzer (TA Instruments make) in presence of nitrogen gas at a heating rate of 20 K/min] of 2,6-dimethylpyridine adsorbed samples. The amount of 2,6-DMP desorbed in the temperature range 573–873 K is taken as the total number BAS

^f RENa–Y is a mixed rare earth exchanged zeolite with La³⁺ as the main counter cation and small amounts of Ce³⁺, Pr³⁺ and Nd³⁺

of Na–Y is 0.18 mmol/g and that of CeNa–Y and LaNa–Y is 0.74 and 0.69 mmol/g respectively. This increase in Brönsted acidity on exchange with rare earth cations is according to several well-established methods of generating BAS in the pores and cavities of zeolites. According to the generally accepted Hirschler–plank mechanism [42], BAS are formed in zeolites containing multivalent cations upon thermal removal of most of the water initially present in the pores. In the local electrostatic field, a water molecule dissociates and proton formed together with negatively charged oxygen framework gives a so-called bridging hydroxyl group that is the catalytically active Brönsted acid site. A slight decrease in the Brönsted acidity in

the case of LaNa–Y must be due to the increased migratory tendency of La³⁺ cations from the large cages to the small cages and subsequent formation of BAS that are not accessible for probe molecules. This observation is in good agreement with the results from silicon-29 MAS NMR and NH₃ TPD studies.

Surface area and pore volume measurements of the parent and various rare earth exchanged zeolite samples are shown in Table 2. The data were reproducible within an error limit of 5%. Surface area and pore volume increase invariably on exchange with rare earth cations. This increase of surface area might be due to the decrease in the crystallite size when sodium form is converted to the rare earth modified forms.

Table 2 Acid structural properties of different systems studied by temperature programmed desorption of ammonia method (373–873 K) and surface area and pore volume measurements

Zeolite	Ammonia desorbed (mmol/g)			Total acid amount	Textural properties		
	W ^{a, b}	M ^b	S ^b		BET surface area (m ² /g)	Langmuir surface area (m ² /g)	Pore volume ^c (cc/g)
Na–Y	0.59	0.12	0.05	0.77	254	389	0.232
CeNa–Y	1.45	0.59	0.20	2.24	484	697	0.296
LaNa–Y	0.92	0.42	0.14	1.48	441	650	0.287
RENa–Y	0.70	0.68	0.46	1.83	468	684	0.291
SmNa–Y	1.21	1.09	0.34	2.64	498	712	0.302
K-10 mont.	0.55	0.24	0.13	0.92	183	304	0.204
SiO ₂ –Al ₂ O ₃	0.55	0.18	0.10	0.83	168	289	0.179

^a Ammonia desorbed in the temperature 373–473 might contain very small amount physisorbed ammonia

^b W, M, and S stand for weak (373–473 K), medium (474–673 K), and strong (674–873 K) acidic sites

^c Total pore volume measured at 0.9976 P/P₀

3.2 Acid sites amount measurements

The acid strength distribution of the parent and various rare earth exchanged zeolites is presented in Table 2. The table describes the distribution of acidity in three temperature regions of 373–473 K (weak acid sites), 473–673 K (medium acid strength) and 673–873 K (strong acid sites). Hence, NH_3 -TPD presents the acid site distribution in zeolites rather than the total acidity. Amount of ammonia desorbed by each sample varies with the nature of rare earth cation present. All the rare earth exchanged samples invariably show high value of acid sites amount. CeNa–Y and SmNa–Y have the maximum acid sites amount and parent Na–Y the least. However, for all the rare earth exchanged zeolites the amount of ammonia desorbed in the high temperature region (673–873 K) is low.

The data on the chemisorption of ammonia in zeolites at different temperatures as obtained from step-wise thermal desorption is presented in Fig. 1. For parent Na–Y and lanthanum exchanged Na–Y zeolite the amount of ammonia-desorbed decrease gradually as the temperature increase. For CeNa–Y, RENa–Y and SmNa–Y zeolites there is increase in the amount of ammonia chemisorbed at 673 K. All zeolites invariably show higher desorption at low temperatures. This is due to the interaction of ammonia with non-acidic or weakly acidic sites in zeolites. The low temperature portion in the case of rare earth exchanged zeolites. This is already reported in the case of mordenite [43]. Hence the number of acid sites measured by the ammonia chemisorption at lower temperature can be taken only as an upper limit of the acid sites in the zeolites. However, at higher temperatures (>623 K) the non-acidic

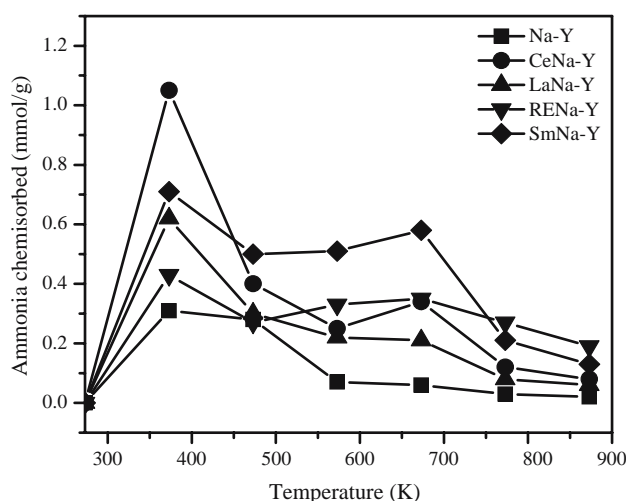


Fig. 1 Temperature dependence of chemisorption of ammonia on parent Na–Y and various rare earth exchanged Na–Y zeolites in the temperature range of 273–873 K

ammonia interactions are weak and hence the sites measured by chemisorption of ammonia are expected to be acidic ones. This part is considerably larger in the case of rare earth exchanged zeolites compared to Na–Y. This supports the enhancement the acid structural properties upon rare earth exchange.

According to the Sanderson's principle of electronegativity equalization, the strength of BAS depends on the nature of cation present and it decrease in the series $\text{HLi-Y} > \text{HNa-Y} > \text{HK-Y}$ [44, 45]. O' Donoghue and Barthomeuf found a decrease of catalytic activity in the dehydration of 2-propanol at 388 K in the same order [44]. Chen et al. interpreted differences in the amount of strongly adsorbed pyridine molecules in zeolites HNa–Y and HK–Y in terms of different strengths of BAS and LAS in these zeolites, i.e., in terms of partial charges residing at the hydrogen and aluminium atoms respectively [45]. Applying the same observation, acid amount should follow the order $\text{SmNa-Y} > \text{CeNa-Y} > \text{LaNa-Y}$. Indeed acid sites amount follows the same order. The specific influence of Ce and Sm is most likely due to the high polarizing power and rather small size (even though in the rare earth series size does not vary much) compared to La, which affects the OH bond through the lattice.

Since in the present systems, a high field shift of silicon-29 MAS NMR signal is already observed upon rare earth exchange of Na–Y zeolite [41], the corresponding cation migration influences the number of multivalent cations that are available for the formation of accessible BAS during thermal treatment. Rare earth migration into the small cages is induced by presence of sodium cations. In rare earth exchanged zeolites, the repulsive interactions of the sodium cations enhance the migration of rare earth cations into small cages. The importance of repulsive interactions for the cation distribution in the small cages of zeolite Y was explained by van Dum and Mortier [46]. A comparative low acid sites amount of LaNa–Y could be due to the presence of large number of La^{3+} ions in the small cages (SI' sites) due to migration.

3.3 Dehydration/Beckmann rearrangement of aldoximes

We have used four classes of solid acid catalysts for the dehydration/Beckmann rearrangement of aldoximes. They are: (1) different rare earth exchanged Na–Y zeolites, (2) H-mordenite zeolite, (3) K-10 montmorillonite clay and (4) amorphous silica-alumina. The reactions have been studied under well-optimized reaction conditions and conducted in a continuous down flow type reactor operated under atmospheric pressure.

3.4 Effect of reaction temperature

The effect of reaction temperature the reaction is examined by performing the synthesis of nitrile or amide at various temperatures under the reaction conditions in the continuous mode maintaining a flow rate of 4 mL/h of oximes (4-methoxybenzaloxime) in a 1:1 mixture of benzene and acetonitrile through the reactor (CeNa–Y zeolite, catalyst loading; 700 mg, reaction time; 3 h). The effect is presented in Fig. 2. As the temperature increases, the conversion of oxime increases. Formation of dehydration product increases whereas production of Beckmann rearrangement product (amide) decreases with an increase in the reaction temperature. This increase is in accordance with a well-documented observation that dehydration increases with temperature. Amide formation via Beckmann rearrangement requires mild temperature conditions and presence of weak acid sites. However, dehydration of aldoximes to corresponding nitriles increases with temperature.

3.5 Comparison of the activities of the catalysts

The results of dehydration/Beckmann rearrangement reactions of benzaldoxime and 4-methoxybenzaloxime are illustrated in Table 3. Benzaldoxime (**1a**) undergo dehydration predominantly, producing benzonitrile

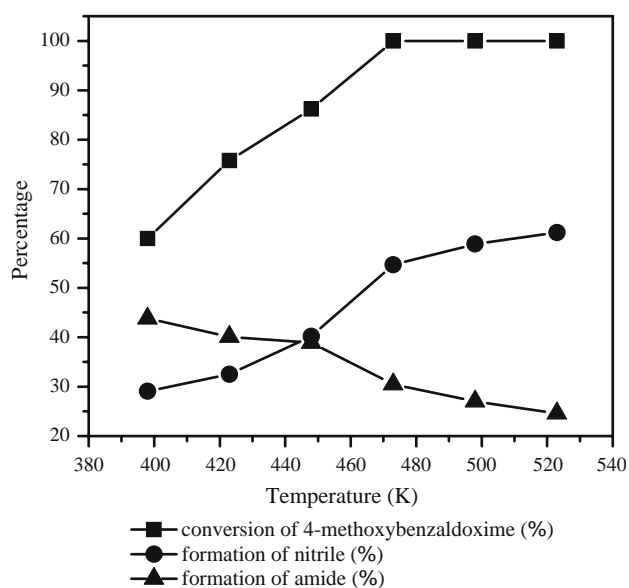


Fig. 2 Conversion of 4-methoxybenzaloxime and formation of nitrile and amide as a function of reaction temperature. Solid acid catalyst: CeNa–Y, catalyst loading: 700 mg, nitrogen flow: 10 mL/h, flow rate: 4 mL/h, time on stream; 2 h, reactant: 5% (w/v) solution of 4-methoxybenzaloxime in 1:1 mixture of benzene-acetonitrile

(**2a**) as the major product in more than 90% yield. Amide formation was not detected in the case of benzaldoxime. However, 4-methoxybenzaloxime (**1b**) yields dehydration as well as Beckmann rearrangement products i.e. 4-methoxybenzonitrile (**2b**) and 4-methoxyphenylformamide (**3**) respectively. In both cases small amounts of oxidation products are also observed. These include; benzaldehyde and benzoic acid with benzaldoxime; 4-methoxybenzaldehyde, 4-methoxybenzoic acid and anisole in the case of 4-methoxybenzaloxime. Rare earth zeolites produce comparatively more amide with 4-methoxybenzaloxime whereas, amide formation was not detected in the case of benzaldoxime. Among different rare earth zeolites, CeNa–Y and RENa–Y produce more byproducts.

Both Beckmann and dehydration reactions are acid catalyzed and has logic to correlate the activity of different catalyst systems with their acid structural properties. Tables 1 and 2 give an idea about the nature of acid sites in rare earth zeolites. In general, rare earth exchanged zeolites have greater acid strength. It is reported that the amount of ammonia desorbed in the medium temperature region is due to BAS [47–49]. Zeolites have greater acid amount in the medium strong acid region (Table 2). Hence zeolites have relatively more number of protonic acid sites than other catalyst systems and consequently show better conversion of aldoximes. SmNa–Y and CeNa–Y zeolites show maximum amount of protonic acid sites as evidenced by 2,6-DMP desorption studies. They also show the maximum cumulative acid amount determined by ammonia TPD studies (Table 2).

Both the aldoximes undergo predominantly dehydration reaction on these zeolites (Table 3). LaNa–Y with its moderate acid amount values (both Brönsted and cumulative) produce dehydration of benzaldoxime (produce 99.5% benzonitrile) and Beckmann rearrangement of 4-methoxybenzaloxime (produce 53.1% 4-methoxyphenylformamide) primarily. Na–Y zeolite with its least acid amount produces maximum amount of 4-methoxyphenylformamide. This is expected as the Beckmann rearrangement requires acid centers of weak strength. Silica-alumina and K-10 montmorillonite with a comparative low BAS shows inferior activity towards the reaction. A similar explanation can be given to the increased amide formation (4-methoxyphenylformamide) over the rare earth exchanged zeolites in the case of 4-methoxybenzaloxime. CeNa–Y and RENa–Y zeolites produce more by-products with both the aldoximes. These side-reaction products include benzaldehyde, benzoic acid (in the case of benzaldoxime) and 4-methoxybenzaldehyde, 4-methoxybenzoic acid and anisole (in the case of 4-methoxybenzaloxime).

Table 3 Dehydration/Beckmann rearrangement^a of aldoximes; benzaldoxime and 4-methoxybenzaldoxime: variation of catalysts

Catalysts	Benzaldoxime conversion selectivity (%)			4-Methoxybenzaldoxime conversion selectivity (%)				
	(%)	Nitrile ^b	Amide ^c	Others ^d	(%)	Nitrile ^e	Amide ^f	Others ^g
Na–Y	78.8	88.8	–	11.2	87.1	30.2	43.4	26.4
CeNa–Y	100	93.9	–	6.1	100	54.7	30.5	14.8
LaNa–Y	100	99.5	–	0.5	98.3	53.1	42.5	4.4
RENa–Y	100	95.7	–	4.3	99.7	54.5	34.3	11.2
SmNa–Y	100	100	–	–	100	61.1	34.8	4.1
H-MOR	100	99.5	–	0.5	99.3	71.3	19.8	8.9
K-10 Mont	78.3	86.9	–	13.1	91.1	51.7	38.6	11.7
SiO ₂ –Al ₂ O ₃	74.0	80.9	–	19.1	90.6	39.4	37.5	23.2

^a Reaction conditions: Temperature: 473 K, Catalyst loading: 700 mg, Reactant: 5% (w/v) solution of oxime in a 1:1 mixture of benzene-acetonitrile, Nitrogen flow: 10 mL/h, Time on stream: 2 h

^b Benzonitrile

^c Phenylformamide

^d Benzaldehyde, benzoic acid and benzene

^e 4-Methoxybenzonitrile

^f 4-Methoxyphenylformamide

^g 4-Methoxybenzaldehyde, 4-Methoxybenzoic acid and anisole

These are all oxidation products and a comparative larger formation of side products on CeNa–Y and RENa–Y (RENa–Y too contains small amount of cerium) might be due to their slight oxidation properties. Among different zeolites, mordenite produce the least amide (with 4-methoxybenzaldoxime). The decreased level of Beckmann rearrangement and a corresponding enhancement in dehydration reaction might be due to its strong acid centers. From the above discussion, we conclude that dehydration needs strong acid sites whereas; Beckmann rearrangement is accomplished over low or medium strength acid sites.

Water is produced during dehydration of aldoximes generating water in the reaction medium. This water is used for the hydrolysis of oximes producing aldehyde in the subsequent stages. Hydrolysis of aldoximes occurred mostly in the late stages of the reaction supporting this observation of generation of water [25, 26, 29, 31]. Partially, the produced water may be responsible for the deactivation of the catalysts as evidenced from time on stream (TOS) studies.

To compare the performance of different rare earth Na–Y zeolites, the dehydration/Beckmann rearrangement reaction have been performed on a series of solid acid catalysts such as H-mordenite, K-10 montmorillonite clay and silica-alumina. H-Mordenite has a bi-directional pore system with parallel circular 12-ring channels (0.65 × 0.70 nm) and elliptical 8-ring channels (0.26 × 0.57 nm) [50]. However, it practically functions as unidirectional pore system as the 8-ring channels are in effect inaccessible for most organic compounds. Cent percentage conversion of aldoximes is observed

on H-mordenite zeolite due to its strong acid structure. Silica-alumina does not have a regular pore structure. K-10 montmorillonite clay is a layered alumino-silicate with an octahedral layer sandwiched between two tetrahedral layers and unlike zeolites, does not have a regular pore structure. However, the average pore size is greater than zeolites (>1.0 nm) [51]. Both silica-alumina and K-10 clay have very weak acid structural properties and hence produce comparatively low conversion of oxime. However, dehydration leading to the formation of nitriles is the predominant reaction on both these catalysts.

3.6 Deactivation, reusability, and heterogeneity studies

The on stream stability of the catalyst systems were tested by performing the synthesis of nitrile or amide under the reaction conditions in the continuous mode for 10 h by maintaining a flow rate of 4 mL/h of oximes (4-methoxybenzaldoxime and benzaldoxime) in a 1:1 mixture of benzene and acetonitrile through the reactor (CeNa–Y or LaNa–Y zeolites, catalyst loading; 700 mg, reaction time; 10 h). The conversion of oximes decreases quickly with reaction time on both the zeolites. Periodic checks by gas chromatography and gas chromatography-mass spectrometer showed this decrease in the total conversion. Figure 3 presents the effect of TOS on the percentage conversion of 4-methoxybenzaldoxime and the selectivity for the formation of amide over CeNa–Y and LaNa–Y. Cent percentage conversion at 2 h of the reaction decreased

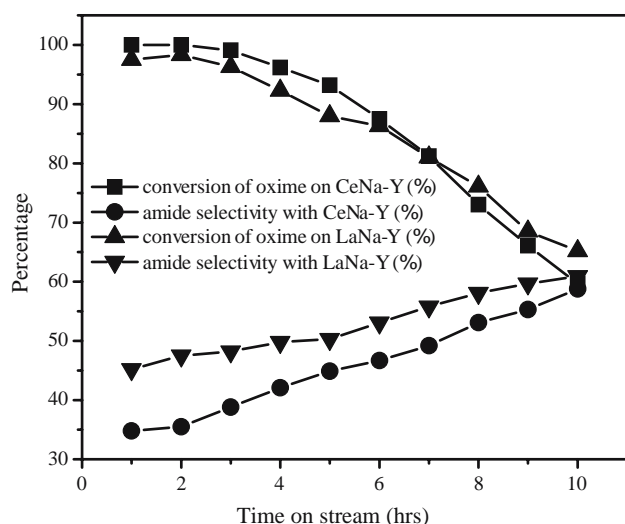


Fig. 3 Effect of time on stream during the dehydration/Beckmann rearrangement reaction of 4-methoxybenzaldoxime on solid acid catalysts: CeNa-Y and LaNa-Y zeolites. Reaction temperature: 473 K, catalyst loading: 700 mg, nitrogen flow: 10 mL/h, flow rate: 4 mL/h, Reactant: 5% (w/v) solution of oxime in 1:1 mixture of benzene-acetonitrile

to 59.7% with CeNa-Y zeolite in 10 h. The corresponding decrease on LaNa-Y was from 98.3 to 60.9% (extent of deactivations were 40.3 and 38.1% respectively for CeNa-Y and LaNa-Y zeolites).

A comparative fast deactivation of CeNa-Y might be due to rather fast neutralization of its strong acid sites. CeNa-Y has more amount of ammonia desorbed in the high temperature domain. However, the selectivity for amide formation (4-methoxyphenylformamide) increases slowly from 35.5 to 58.8% in an equal TOS on CeNa-Y zeolite (47.5 to 60.9% on LaNa-Y zeolite). The deactivation of catalysts is generally due to the formation and trapping in the zeolite pores of secondary products of the reaction [52, 53] (called coke for sake of simplification). In the present case the deactivation of the catalyst is due to the neutralization of acid sites (very strong interaction between the active centers and the basic molecules) by the basic reactant and product molecules (oxime and amide). However, the formation of amide (Beckmann rearrangement) increases upon deactivation. This could be explained by considering the fact that the dehydration reaction needs strong acid centers whereas, mild or even weak acid sites can effect Beckmann rearrangement of oximes. This is supported by the performance of CeNa-Y zeolite, which is more acidic than LaNa-Y zeolite and produces more dehydration. As most of the acid sites getting deactivated during the course of reaction by reactants and products, the dehydration become nominal and at the same time the probability of Beckmann rearrangement increases slightly. Comparative greater

stability of LaNa-Y zeolite is due its moderate acid amount as evidenced by 2,6-DMP thermodesorption and TPD studies. These mild acid centers undergo slow poisoning with basic reactants and products.

A similar trend is observed during the TOS studies of benzaldoxime with CeNa-Y and LaNa-Y zeolites as seen in Fig. 4. The conversion of oxime decreases with time on both the zeolites. The activity decreases from cent percentage to 74% for CeNa-Y and from 100 to 77.5% with LaNa-Y. Thus, CeNa-Y and LaNa-Y underwent 26 and 22.5% deactivation in 10 h. Amide formation was not detected during the early stages of reaction on both the catalysts. However, it was formed at later stages and formation of amide increase with reaction time. CeNa-Y produces 5.3% and LaNa-Y 7.4% at the end of the reaction. As most of the acid sites getting deactivated, dehydration becomes less efficient, while the probability of Beckmann rearrangement increases. The amount of coke formed during the reaction was 21% ($\pm 5\%$) after 10 h over CeNa-Y zeolite. The coke should be composed of reactants and various reaction products especially the polymeric products which are trapped inside the zeolite pores.

The variation of the reaction conversion on repeated usage of the catalysts was checked. The Langmuir surface area of the regenerated CeNa-Y and LaNa-Y zeolites were 689 and 642 m^2/g respectively. This value is almost the same as that of the original zeolites (Table 2) and this rule out any structural changes during the catalytic reaction. When the catalyst is used

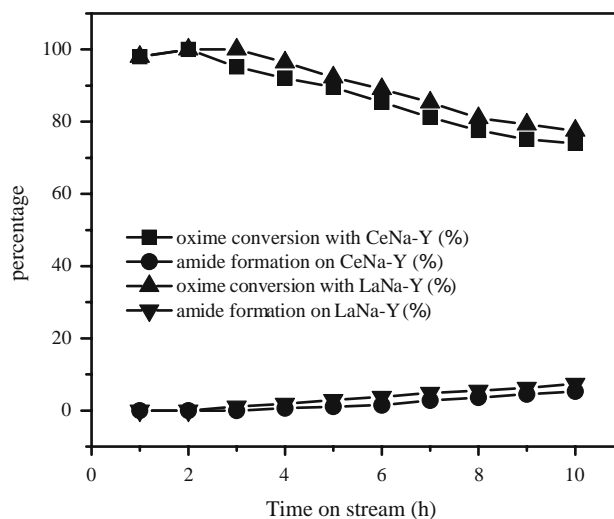


Fig. 4 Effect of time on stream on the dehydration/Beckmann rearrangement reaction of benzaldoxime on solid acid catalysts: CeNa-Y and LaNa-Y zeolites. Reaction temperature: 473 K, catalyst loading: 700 mg, nitrogen flow: 10 mL/h, flow rate: 4 mL/h, Reactant: 5% (w/v) solution of oxime in 1:1 mixture of benzene-acetonitrile

for the first time, cent percentage conversion of oxime was observed on CeNa–Y, while 98.3% conversion over LaNa–Y zeolite. However, on second usage (after continuous extraction with DCM followed by oxidative treatment at 773 K), the reaction conversion was 99.1 and 97.6% respectively for CeNa–Y and LaNa–Y zeolites. When reused for the third time 98.1 and 95.6% conversion was obtained for the two zeolites. Deactivation/regeneration results show that the solid acid catalysts could be regenerated and reused effectively. TOS studies show that the catalysts when fresh, deactivated quickly. When some coke is deposited on the catalyst, the rate of deactivation decreases. Since there is no waste formation in the reaction, the *E-factor* must be low and *atom efficiency* high. In conclusion, a simple, efficient, and highly environmentally friendly protocol is described for the production of nitriles and amides (in the case of 4-methoxy benzaldoxime).

We have performed studies to obtain clear evidence for the true heterogeneity and stability of the catalytic systems. The reaction mixture was passed through CeNa–Y and H-MOR zeolites under standard reaction conditions for 10 h. No aluminium was detected in the reaction mixture by the Energy Dispersive X-ray analysis. Furthermore, aluminium was not detected during qualitative chemical analysis of the reaction mixture. These results strongly rule out the possibility of aluminium leaching during the reaction.

3.7 Mechanism of the reaction

Benzaldoxime (**1a**, mp 308 K, *syn*-isomer) and 4-methoxybenzaldoxime (**1b**, mp 339–340 K, *syn*-isomer) were prepared using standard procedures [54]. A plausible mechanism for the formation of various products is presented in Fig. 5. The oxime molecules (**1a** and **1b**) adsorbed to the catalyst surface are efficiently protonated to give **2**. Dehydration of **2** over the catalyst surface will lead to the formation of nitriles **3**. Alternatively, migration of anti-aryl group to nitrogen

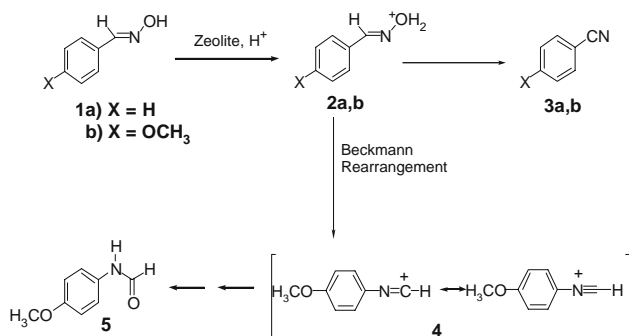


Fig. 5 Scheme showing the possible mechanism of the reaction

concomitant with the removal of a molecule of water will lead to the resonance stabilized intermediate **4**. Further transformation of **4** (addition of water followed by tautomerization) will lead to amide **5**. The difference in chemoselectivity exhibited by benzaldoxime (**1a**) and 4-methoxybenzaldoxime (**1b**) is explainable on the basis of electronic factors. We conclude that the electron-donating 4-methoxyphenyl group stabilizes intermediates such as **2b** and **4** over **2a**. Furthermore, based on detailed kinetic analysis, Gregory co-workers [55] have established that substituent effects (as illustrated by the linear relationship existing between the Hammett σ^+ values and observed rate constants) are important for Beckmann rearrangement involving aryl migration. The rate of migration of 4-methoxyphenyl group is estimated at 3 to 4 times higher than that of phenyl groups.

4 Conclusion

In this paper a novel application of solid acid catalysts in the dehydration/Beckmann of rearrangement aldoximes is reported. The optimal protocol allows the nitriles and amides to be synthesised in excellent yields. Na–Y, rare earth exchanged Na–Y, H-mordenite zeolites, K-10 montmorillonite clay and amorphous silica-alumina have been effectively employed for the reaction. Benzonitrile was obtained in (near) quantitative yields by the dehydration of benzaldoxime over these catalysts. 4-Methoxybenzaldoxime gave both Beckmann rearrangement product (4-methoxyphenylformamide) and dehydration product (4-methoxybenzonitrile) in high overall yields. In conclusion, a novel procedure for zeolites catalyzed dehydration/Beckmann rearrangement of aldoximes for the synthesis of nitriles and amides is described. Examples of highly atom economic practical continuous mode reactions are presented by using common laboratory down flow type reactor and mild experimental conditions. These preliminary results, in principle, afford an effective substitute for the high temperature ammoxidation type reactions for the synthesis nitriles and studies addressed towards the extension of this protocol to other aldoximes are actually under investigation.

Acknowledgments The aldoximes and authentic samples of nitriles employed in this study were prepared by undergraduate students of this department as part of their Organic Chemistry Laboratory course. The authors are grateful to Dr. C. V. Asokan, School of Chemical Sciences, Mahatma Gandhi University, Kottayam for providing the GC-MS results. B. Thomas is grateful to Council of Scientific and Industrial Research for Senior Research Fellowship.

References

1. M. Ikemoto, K. Tsutsumi, H. Takabashi, Bull. Chem. Soc. Jpn. **45**, 1330 (1972)
2. P.B. Venuto, E.T. Habib Jr., in *Fluid Catalytic Cracking with Zeolite Catalysts* (Marcel Dekker, New York, 1979)
3. M.L. Occelli (ed.) in *Fluid Catalytic Cracking* (Am. Chem. Soc. Washington, DC, 1988)
4. K. Becker, K.H. Steinberg, H. Bremer, V. Kanazirev, Ch. Dimitrov, K. Nestler, C.M. Minacev, Chem. Tech. **23**, 296 (1981)
5. K. Tanabe, W.F. Holdrich, Appl. Catal. A: Gen. **181**, 399 (1999)
6. S. Sivasanker, A. Thangaraj, J. Catal. **138**, 386 (1992)
7. G.A. Olah, in *Friedel-Crafts and Related Reactions*, vol. 1 (Wiley Interscience, New York, 1963)
8. H. Sato, N. Ishii, K. Hirose, S. Nakamura, Stud. Surf. Sci. Catal. **28**, 755 (1986)
9. Z. Rappoport, in *Chemistry of Cyano Group* (John Wiley and Sons, London, 1970)
10. J. March, in *Advanced Organic Chemistry—Reactions, Mechanisms, and Structure*, 4th edn. (John Wiley and Sons, 1992) p. 1041
11. L.C. Larock (ed.), in *Comprehensive Organic Transformation. A Guide to Functional Group Preparation* (VCH Inc., New York, 1989) p. 991
12. P.J. Stobbelaar, Ph.D. Thesis, University of Eindhoven, (2000)
13. K.N. Reddy, Weed Technol. **18**(1), 131 (2004)
14. B.N. Naidu, M.E. Sorenson, Org. Lett. **7**(7), 1391 (2005)
15. G.A. Olah, in *Friedel-Crafts Chemistry*, vol. 1 (Wiley; New York, 1963) p. 119
16. K. Adachi, T. Sugawara, Synth. Commun. **20**, 71 (1990)
17. F. Cavani, F. Trifiro, J. Mol. Catal. A: Chem. **43**, 117 (1987)
18. P. Cavalli, F. Cavani, T. Manenti, F. Trifiro, Ind. Eng. Chem. Res. **26**, 679 (1987)
19. M. Sanati, A. Andersson, L.R. Wallenberg, B. Rebenstorf, Appl. Catal. A: Gen. **196**, 51 (1993)
20. K.V.R. Chary, C. P. Kumar, A. Murali, A. Tripathi, A. Clearfield, J. Mol. Catal. A: Chem. **216**, 139 (2004)
21. C.P. Kumar, K.R. Reddy, V.V. Rao, K.V.R. Chary, Green Chem. **4**, 513 (2002)
22. M.N. Rao, P. Kumar, K. Garyali, Org. Prep. Proced. Int. **21**, 230 (1989)
23. H.M. Meshram, Synthesis **10**, 943 (1992)
24. E. Gutierrez, A.J. Aznar, E. Ruiz-Hitzky, Stud. Surf. Sci. Catal. **59**, 539 (1991)
25. S. Sato, S. Hasebe, H. Sakurai, K. Urabe, Y. Izumi, Appl. Catal. A: Gen. **29**, 107 (1987)
26. S. Sato, K. Urabe, Y. Izumi, J. Catal. **102**, 99 (1986)
27. A. Costa, P.M. Deya, J.V. Sinisterra, J.M. Marinas, Can. J. Chem. **58**, 1266 (1980)
28. H.M. Meshram, Synth. Commun. **20**, 3253 (1990)
29. P.S. Landis, P.B. Venuto, J. Catal. **6**, 245 (1986)
30. M.C. Burguet, A. Aucejo, A. Corma, Can. J. Chem. Eng. **65**, 944 (1987)
31. A. Aucejo, M.C. Burguet, A. Corma, V. Fornes, Appl. Catal. **22**, 187 (1986)
32. A. Thangaraj, S. Sivasanker, P. Ratnasamy, J. Catal. **252**, 137 (1991)
33. J.S. Reddy, R. Ravishankar, S. Sivasanker, P. Ratnasamy, Catal. Lett. **17**, 139 (1993)
34. B. Thomas, S. Prathapan, S. Sugunan, Appl. Catal. A: Gen. **277**, 247 (2004)
35. B. Thomas, S. Prathapan, S. Sugunan, in *Proceedings of the 3rd International Zeolite Symposium*, Prague, Stud. Surf. Sci. Catal. (in press)
36. P.K. Dutta, R.E. Zaykoski, M.A. Thomson, Zeolites **6**, 423 (1986)
37. R. Carvajal, P.-J. Chu, J.H. Lunsford, J. Catal. **125**, 123 (1990)
38. N.N. Greenwood, A. Earnshaw, in *Chemistry of the Elements*, 2nd edn. (Butterworth-Heinemann, Oxford, 1997) p. 345
39. F.A. Cotton, G. Wilkinson, C.A. Murillo, M. Bochmann, in *Advanced Inorganic Chemistry*, 6th edn. (John Wiley and Sons Inc., New York, 1999) p. 178
40. R.A. Jonathan, N. Pervaiz, A.K. Cheetham, M.W. Anderson, J. Am. Chem. Soc. **120**, 10754 (1998)
41. B. Thomas, S. Sugunan, Micropor. Mesopor. Mater. **72**, 227 (2004)
42. A.E. Hirschler, J. Catal. **2**, 428 (1963)
43. S.G. Pataskar, PhD thesis University of Poona, Pune, (1984)
44. E.O' Donoghue, D. Barthomeuf, Zeolites **6**, 267 (1986)
45. Y.S. Chen, M. Guisnet, M. Kern, J.L.K. Lemberston, New J. Chem. **11**, 623 (1987)
46. J. van Dum, W.J. Mortier, J. Phys. Chem. **92**, 6740 (1988)
47. J. Catanach, E.L. Wu, P.B. Venuto, J. Catal. **11**, 342 (1968)
48. A. Corma, V. Fornes, F.W. Melo, J. Herrero, Zeolites **7**, 559 (1987)
49. B.M. Lok, B.K. Marcus, C.L. Angell, Zeolites **6**, 185 (1986)
50. W.M. Meier, Z. Kristallogr. **115**, 439 (1961)
51. A.V. Ramaswamy, Sci. Tech. Chimica & Industria, **1** (2000)
52. M. Guisnet, P. Magnoux, Appl. Catal. **54**, 1 (1989)
53. S. Sivasanker, *Catalyst Deactivation* (ed.), B. Viswanathan, S. Sivasanker, A.V. Ramaswamy, in *Catalysis Principles and Applications*, (Narosa Publishing House, New Delhi, 2002) p. 253
54. D.B. Dalton, H.G. Foley, J. Org. Chem. **38**, 4200 (1973)
55. B.J. Gregory, R.B. Moodie, K. Schofield, J. Am. Chem. Soc. **13**, 338 (1970)